Open Heavy Flavor Studies for the ECCE Detector at the Electron Ion Collider

X. Li[31], J. K. Adkins[35], Y. Akiba[52], A. Albataineh[68], M. Amaryan[46], I. C. Arsene[72], J. Bae[60], X. Bai[77], M. Bashkanov[86], R. Bellwied[66], F. Benmokhtar[14], J. C. Bernauer[54,55,56], F. Bock[48], W. Boeglin[16], M. Borysova[82], E. Brash[10], P. Brindza[27], W. J. Briscoe[20], M. Brooks[31], S. Bueltmann[46], M. H. S. Bukhari[26], A. Bylinkin[68], R. Capobianco[65], W.-C. Chang[2], Y. Cheon[58], K. Chen[7], K.-F. Chen[45], K.-Y. Cheng[39], M. Chiu[4], T. Chujo[75], Z. Citron[1], E. Cline[54,55], E. Cohen[43], T. Cormier[48], Y. Corrales Morales[31], C. Cotton[77], C. Crawford[69], S. Creekmore[48], C.Cuevas[27], J. Cunningham[48], G. David[4], C. T. Dean[31], M. Demarteau[48], S. Diehl[65], N. Doshita[84], R. Dupré[23], J. M. Durham[31], R. Dzhygadlo[19], R. Ehlers[48], L. El Fassi[37], A. Emmert[77], R. Ent[27], C. Fanelli[36], R. Fatemi[69], S. Fegan[86], M. Finger[8], M. Finger Jr.[8], J. Frantz[47], M. Friedman[22], I. Friscic[87], D. Gangadharan[66], S. Gardner[18], K. Gates[18], F. Geurts[51], R. Gilman[53], D. Glazier[18], E. Glimos[48], Y. Goto[52], N. Grau[3], S. V. Greene[78], A. Q. Guo[24], L. Guo[16], S. K. Ha[85], J. Haggerty[4], T. Hayward[65], X. He[17], O. Hen[36], D. W. Higinbotham[27], M. Hoballah[23], P.-h. J. Hsu[44], J. Huang[4], G. Huber[73], A. Hutson[66], K. Y. Hwang[85], C. Hyde[46], M. Inaba[63], T. Iwata[84], H.-S. Jo[30], K. Joo[65], N. Kalantarians[80], K. Kawade[59], S. Kay[73], A. Kim[65], B. Kim[60], C. Kim[50], M. Kim[52], Y. Kim[50], Y. Kim[58], E. Kistenev[4], V. Klimenko[65], S. H. Ko[57], I. Korover[36], W. Korsch[69], G. Krintiras[68], S. Kuhn[46], C.-M. Kuo[39], T. Kutz[36], J. Lajoie[25], D. Lawrence[27], S. Lebedev[25], J. S. H. Lee[57], S. W. Lee[30], Y.-J. Lee[36], W. Li[51], W. Li[54,55,83], X. Li[9], Y. T. Liang[24], S. Lim[50], C.-h. Lin[2], D. X. Lin[24], K. Liu[31], M. X. Liu[31], K. Livingston[18], N. Liyanage[77], W. J. Llope[81], C. Loizides[48], E. Long[71], R.-S. Lu[45], Z. Lu[9], W. Lynch[86], D. Marchand[23], M. Marcisovsky[13], P. Markowitz[16], P. McGaughey[31], M. Mihovilovic[70], R. G. Milner[36], A. Milov[82], Y. Miyachi[84], P. Monaghan[10], R. Montgomery[18], D. Morrison[4], C. Munoz Camacho[23], M. Murray[68], K. Nagai[31], J. Nagle[64], I. Nakagawa[52], C. Nattrass[76], D. Nguyen[27], S. Niccolai[23], R. Nouicer[4], G. Nukazuka[52], M. Nycz[77], V. A. Okorokov[42], S. Orešić[73], J. Osborn[48], C. O'Shaughnessy[31], S. Paganis[45], Z Papandreou[73], S. Pate[41], M. Patel[25], C. Paus[36], G. Penman[18], M. G. Perdekamp[67], D. V. Perepelitsa[64], H. Periera da Costa[31], K. Peters[19], W. Phelps[10], E. Piasetzky[61], C. Pinkenburg[4], I. Prochazka[8], T. Protzman[33], M. Purschke[4], J. Putschke[81], J. R. Pybus[36], R. Rajput-Ghoshal[27], J. Rasson[48], B. Raue[16], K. Read[48], K. Røed[72], R. Reed[33], J. Reinhold[16], E. L. Renner[31], J. Richards[65], C. Riedl[67], T. Rinn[4], J. Roche[47], G. M. Roland[36], G. Ron[22], M. Rosati[25], C. Royon[68], J. Ryu[50], S. Salur[53], N. Santiesteban[36], R. Santos[65], M. Sarsour[17], J. Schambach[48], A. Schmidt[20], N. Schmidt[48], C. Schwarz[19], J. Schwiening[19], R. Seidl[52], A. Sickles[67], P. Simmerling[65], S. Sirca[70], D. Sharma[17], Z. Shi[31], T.-A. Shibata[40], C.-W. Shih[39], S. Shimizu[52], U. Shrestha[65], K. Slifer[71], K. Smith[31], R. Soltz[34], W. Sondheim[31], J. Song[9], J. Song[50], I. I. Strakovsky[20], P. Steinberg[4], J. Stevens[83], J. Strube[49], P. Sun[9], X. Sun[7], K. Suresh[73], W.-C. Tang[39], S. Tapia Araya[25], S. Tarafdar[78], L. Teodorescu[5], A. Timmins[66], L. Tomasek[13], N. Trotta[65], T. S. Tveter[72], E. Umaka[25], A. Usman[73], H. W. van Hecke[31], J. Velkovska[78], E. Voutier[23], P.K. Wang[23], Q. Wang[68], Y. Wang[7], Y. Wang[62], D. P. Watts[86], L. Weinstein[46], M. Williams[36], C.-P. Wong[31], L. Wood[49], M. H. Wood[6], C. Woody[4], B. Wyslouch[36], Z. Xiao[62], Y. Yamazaki[29], Y. Yang[38], Z. Ye[62], H. D. Yoo[85], M. Yurov[31], N. Zachariou[86], W.A. Zajc[11], J. Zhang[77], Y. Zhang[62], Y. X. Zhao[24], X. Zheng[77], P. Zhuang[62]

[1]A. Alikhanyan National Laboratory, Yerevan, Armenia
[2]Institute of Physics, Academia Sinica, Taipei, Taiwan
[3]Augustana University, , Sioux Falls, , SD, USA
[4]Brookhaven National Laboratory, , Upton, 11973, NY, USA
[5]Brunel University London, , Uxbridge, , UK
[6]Canisius College, , Buffalo, , NY, USA
[7]Central China Normal University, Wuhan, China
[8]Charles University, Prague, Czech Republic
[9]China Institute of Atomic Energy, Fangshan, Beijing, China
[10]Christopher Newport University, , Newport News, , VA, USA
[11]Columbia University, , New York, , NY, USA
[12]Catholic University of America, 620 Michigan Ave., Washington DC, 20064, USA
[13]Czech Technical University, , Prague, Czech Republic
[14]Duquesne University, , Pittsburgh, , PA, USA
[15]Duke University, , , , NC, USA
[16]Florida International University, , Miami, , FL, USA
[17]Georgia State University, , Atlanta, , GA, USA
[18]University of Glasgow, , Glasgow, , UK
[19]GSI Helmholtzzentrum fuer Schwerionenforschung, , Darmstadt, , Germany
[20]The George Washington University, , Washington, DC, , USA
[21]Hampton University, , Hampton, , VA, USA
[22]Hebrew University, , Jerusalem, , Isreal
[23]Universite Paris-Saclay, CNRS/IN2P3, IJCLab, Orsay, France
[24]Chinese Academy of Sciences, , Lanzhou, , , China
[25]Iowa State University, , , , IA, USA
[26]Jazan University, Jazan, Sadui Arabia
[27]Thomas Jefferson National Accelerator Facility, 12000 Jefferson Ave., Newport News, 24450, VA, USA
[28]James Madison University, , , , VA, USA

[29]Kobe University, Kobe, Japan
[30]Kyungpook National University, Daegu, Republic of Korea
[31]Los Alamos National Laboratory, , , , NM, USA
[32]Lawrence Berkeley National Lab, , Berkeley, , , USA
[33]Lehigh University, , Bethlehem, , PA, USA
[34]Lawrence Livermore National Laboratory, , Livermore, , CA, USA
[35]Morehead State University, Morehad, KY, USA, , Morehead, , KY, USA
[36]Massachusetts Institute of Technology, 77 Massachusetts Ave., Cambridge, 02139, MA, USA
[37]Mississippi State University, , Mississippi State, , MS, USA
[38] National Cheng Kung University, Tainan, Taiwan, , , , ,
[39]National Central University, Chungli, Taiwan
[40]Nihon University, Tokyo, Japan
[41]New Mexico State University, , Las Cruces, , NM, USA
[42]National Research Nuclear University MEPhI, Moscow, Russian Federation
[43]Nuclear Research Center - Negev, Beer-Sheva, Isreal
[44]National Tsing Hua University, Hsinchu, Taiwan
[45]National Taiwan University, Taipei, Taiwan
[46]Old Dominion University, , Norfolk, , VA, USA
[47]Ohio University, , Athens, , OH, USA
[48]Oak Ridge National Laboratory, PO Box 2008, Oak Ridge, 37831, TN, USA
[49]Pacific Northwest National Laboratory, , Richland, , WA, USA
[50]Pusan National Univeristy, Busan, Republic of Korea
[51]Rice University, P.O. Box 1892, Houston, 77251, TX, USA
[52]RIKEN Nishina Center, Wako, Saitama, Japan
[53]The State University of New Jersey, , Piscataway, , NJ, USA
[54]Center for Frontiers in Nuclear Science, Stony Brook, 11794, NY, USA
[55]Stony Brook University, 100 Nicolis Rd., Stony Brook, 11794, NY, USA
[56]RIKEN BNL Research Center, , Upton, , NY, USA
[57]Seoul National University, Seoul, Republic of Korea
[58]Sejong University, Seoul, Republic of Korea
[59]Shinshu University, Matsumoto, Nagano, Japan
[60]Sungkyunkwan University, Suwon, Republic of Korea
[61]Tel Aviv University, P.O. Box 39040, Tel Aviv, 6997801, Israel
[62]Tsinghua University, Beijing, China
[63]Tsukuba University of Technology, Tsukuba, Ibaraki, Japan
[64]University of Colorado Boulder, Boulder, CO, USA, , Boulder, , CO, USA
[65]University of Connecticut, , Boulder, Storrs, , CT, USA
[66]University of Houston, , Houston, , TX, USA
[67]University of Illinois, , Urbana, , IL, USA
[68]Unviersity of Kansas, 1450 Jayhawk Blvd., Lawrence, 66045, KS, USA
[69]University of Kentucky, , Lexington, 40506, KY, USA
[70]University of Ljubljana, Ljubljana, Slovenia, , Ljubljana, , , Slovenia
[71]University of New Hampshire, , Durham, , NH, USA
[72]University of Oslo, Oslo, Norway
[73] University of Regina, , Regina, , SK, Canada
[74]University of Seoul, Seoul, Republic of Korea
[75]University of Tsukuba, Tsukuba, Japan
[76]University of Tennessee, , Knoxville, , TN, USA
[77]University of Virginia, , Charlottesville, , VA, USA
[78]Vanderbilt University, , Nashville, , TN, USA
[79]Virginia Tech, , Blacksburg, , VA, USA
[80]Virginia Union University, , Richmond, , VA, USA
[81]Wayne State University, , Detroit, , MI, USA
[82]Weizmann Institute of Science, Rehovot, Israel
[83]The College of William and Mary, Williamsburg, VA, USA
[84]Yamagata University, Yamagata, Japan
[85]Yarmouk University, Irbid, Jordan
[86]Yonsei University, Seoul, Republic of Korea
[87]University of York, York, UK
[88]University of Zagreb, Zagreb, Croatia

Abstract

The ECCE detector has been recommended as the selected reference detector for the future Electron-Ion Collider (EIC). A series of simulation studies have been carried out to validate the physics feasibility for the ECCE detector. In this paper, detailed studies of heavy flavor hadron and jet reconstruction and cross section projections with the ECCE detector performance and different magnet

options will be presented. The broad kinematic coverage and better precision enabled by the proposed EIC heavy flavor hadron and jet measurements will help explore the hadronization process in vacuum and nuclear medium.

Keywords: ECCE, Electron Ion Collider, Tracking, Heavy Flavor

Contents

1. Introduction

The EIC yellow report [1] has listed several fundamental questions which will be resolved/explored at the future EIC. How colored quarks and gluons form into the the colorless matter, which is known as the hadronization process, is one of the EIC primary science objectives. The future EIC will operate high luminosity and high energy $e + p$ and $e + A$ collisions with the instant luminosity at $10^{33-34} cm^{-2} s^{-1}$ and a variety of center of mass energy from 20 GeV to 141 GeV. This will create an ideal environment to explore the hadornization process in vacuum and a nuclear medium.

This paper summarizes the latest simulation studies for reconstructed heavy flavor hadrons and jets in $e + p$ collisions and the corresponding nuclear modification factor projections in $e+p$ and $e+Au$ collisions. The selected collision combination is 10 GeV electron and 100 GeV proton/nucleus, which is projected to reach the highest $e+A$ energy combination at the future EIC. Latest ECCE conceptual design has been implemented in the GEANT4 simulation. Heavy flavor reconstruction has been studied in PYTHIA8 simulation with the latest EIC accelerator design and ECCE detector performance. The content includes the simulation configuration, heavy flavor reconstruction analysis procedure, physics projection and summary.

2. Simulation Setup

2.1. Analysis Framework

The simulation framework for the heavy flavor hadron and jet reconstruction includes event generation in PYTHIA8.2 [2], ECCE tracking detector performance extrapolated in Fun4All based GEANT4 [3], parameterized detector performance of PID, EMCal and HCal discussed in section 3 and 11 in the EIC yellow report. 60 M events have been generated in PYTHIA 8.240 with $Q^2_{min} = 10 Gev/c^2$ and heavy flavor hadron decay channel on. The pythia8 configuration setup is the following:

- PhaseSpace:Q2Min = 10
- WeakBosonExchange:ff2ff(t:gmZ) = on
- WeakBosonExchange:ff2ff(t:W) = on
- SpaceShower:dipoleRecoil = on
- heavy flavor hadorn decay channel on, for example: 413:onMode = on.

These high Q^2 events have been first scaled with minimum bias events and then scaled with the integrated luminosity.

With several iterations of detector design updates, integration with different ECCE subsystems, and implementation of the service mechanical structure, the ECCE tracking detector geometry has been finalized. The silicon vertex/tracking detector is essential to realized the proposed heavy flavor measurements. The silicon barrel subsystem inherited from the EIC silicon consortium design [4] and detailed parameters are shown in Table 1. The LANL EIC team is developing a heavy flavor and jet physics program for the furture EIC [5], a proposed Forward Silicon Tracker (FST) detector design and R&D is part of this program. Recent FST detector design including the conceptual support structure and cooling distributions have been included in the ECCE silicon vertex/tracking subsystem [6]. Detailed design parameters for the silicon hadron endcap detector are shown in Table 2 and the corresponding geometry parameters for the electron endcap detector are shown in Table 3.

Layer index	technology	radius	minimum z	maximum z	pixel pitch
1	MAPS	3.3 cm	-13.5 cm	13.5 cm	10 μm
2	MAPS	4.35 cm	-13.5 cm	13.5 cm	10 μm
3	MAPS	5.4 cm	-13.5 cm	13.5 cm	10 μm
4	MAPS	21.0 cm	-27 cm	27 cm	10 μm
5	MAPS	22.68 cm	-30 cm	30 cm	10 μm

Table 1: The ECCE silicon barrel detector conceptual design geometry.

Disk index	technology	z location	inner radius	outer radius	pixel pitch
1	MAPS	-25 cm	3.5 cm	18.5 cm	10 μm
2	MAPS	-52 cm	3.5 cm	36.5 cm	10 μm
3	MAPS	-79 cm	4.5 cm	40.5 cm	10 μm
4	MAPS	-106 cm	5.5 cm	41.5 cm	10 μm

Table 2: The ECCE silicon electron endcap detector conceptual design geometry.

Disk index	technology	z location	inner radius	outer radius	pixel pitch
1	MAPS	25 cm	3.5 cm	18.5 cm	10 μm
2	MAPS	49 cm	3.5 cm	36.5 cm	10 μm
3	MAPS	73 cm	4.5 cm	40.5 cm	10 μm
4	MAPS	106 cm	5.5 cm	41.5 cm	10 μm
5	MAPS	125 cm	7.5 cm	43.5 cm	10 μm

Table 3: The ECCE silicon hadron endcap detector conceptual design geometry.

Using the single pion events from the 3rd simulation production, the evaluated tracking momentum resolutions are shown

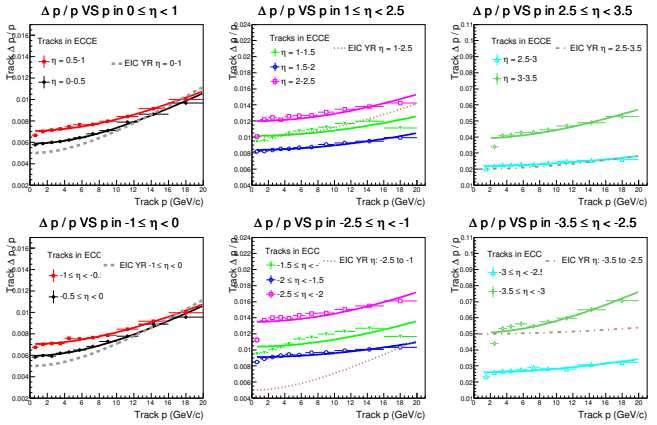

Figure 1: Track momentum dependent momentum resolution in $0 \leq \eta \leq 3.5$ and $-3.5 \leq \eta < 0$ pseudorapidity regions.

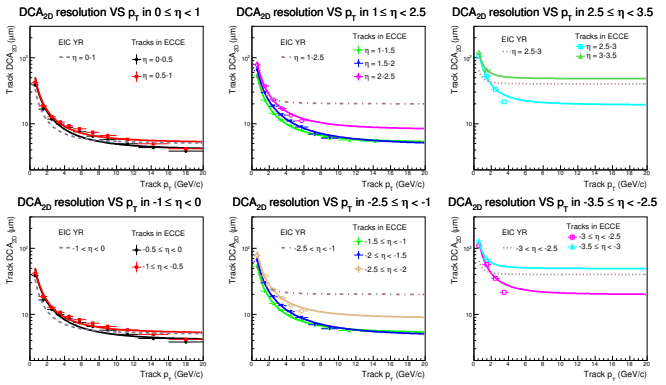

Figure 2: Track momentum dependent momentum resolution in $0 \leq \eta \leq 3.5$ and $-3.5 \leq \eta < 0$ pseudorapidity regions.

in FIG 1 and transverse DCA (DCA_{2D}) resolutions are shown in FIG 2.

These tracking performance have been parameterized with the fit function defined in the EIC yellow report and implement in the PYTHIA 8 simulation.

2.2. *Open Heavy Flavor Hadron and Jet Reconstruction*

To reconstructed heavy flavor hadrons, a list of cuts have been applied:

- DCA_{2D} matching between charged tracks within 2 sigma separation of the DCA_{2D} resolutions (in general, the $\Delta DCA_{2D} < 100\mu m$).
- Each charged track transverse momentum $p_T > 0.2 GeV/c$.
- Reconstructed heavy flavor hadron DCA and momentum angle θ, $cos(\theta^*) > 0.25$.

Reconstructed heavy flavor hadrons including have been successfully reconstructed in 10+100 GeV $e+p$ collisions. Clear signals of $D^{\pm}$, $D^0(\bar{D}^0)$, $D_s^{\pm}$, $\Lambda_c^{\pm}$, $B^{\pm}$, $B^0(\bar{B}^0)$ have been found on top of the combinatorial background. It's a bit challenging to search for $B_s^0(\bar{B}_s^0)$ signals with the current ECCE detector configuration and around one year EIC data collection. Reconstructed D^0 ($\bar{D}^0$) in four different pseudorapidity regions in 10+100 GeV e+p collisions with $10 fb^{-1}$ integrated luminosity are shown in Figure 4.

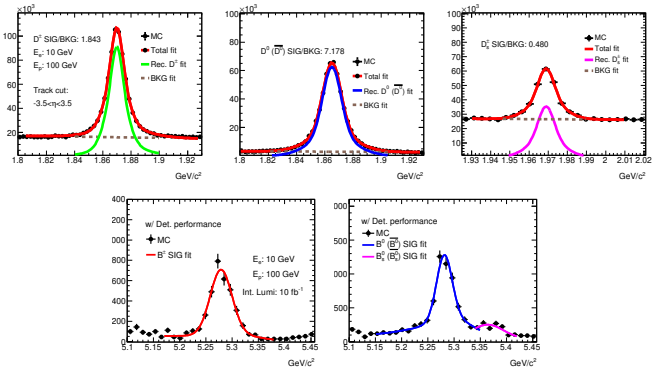

Figure 3: Reconstructed heavy flavor hadrons with the ECCE detector performance in 10+100 GeV $e+p$ collisions. The integrated luminosity is 10 fb^{-1}.

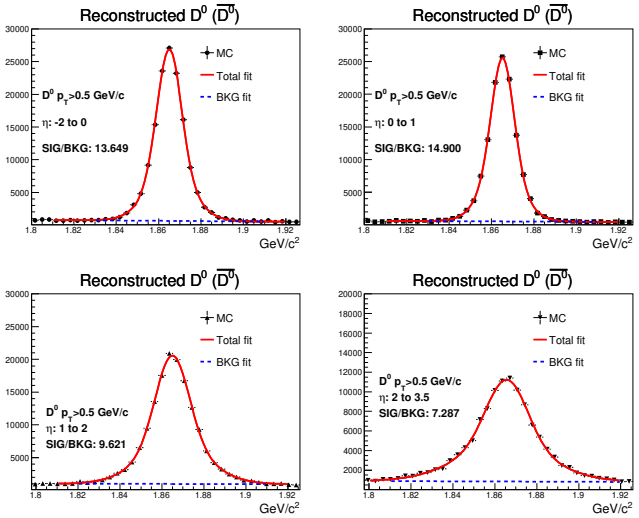

Figure 4: Reconstructed heavy flavor hadrons with the ECCE detector performance in 10+100 GeV $e+p$ collisions. The integrated luminosity is 10 fb^{-1}.

D^0 ($\bar{D}^0$) reconstruction purity and the acceptance*efficiency have been evaluated in three different pseudorapidity regions, which are $-2 < \eta \leq 0$, $0 < \eta \leq 2$ and $2 < \eta \leq 3.5$. The purity is defined as the yields of reconstructed D^0 ($\bar{D}^0$) associated with true particles divided by the reconstructed D^0 ($\bar{D}^0$) yields. The acceptance by efficiency is defined as the reconstructed D^0 ($\bar{D}^0$) yields divided by the generated D^0 ($\bar{D}^0$) yields. The purity and reconstruction acceptance*efficiency for transverse momentum dependent reconstructed D^0 ($\bar{D}^0$) in e+p simulation are illustrated in Figure 5. The distributions are studied with track transverse momentum $0.5\ GeV/c < p_T < 7\ GeV/c$ in three different pseudorapidity regions: $-2 < \eta \leq 0$, $0 < \eta \leq 2$,

$2 < \eta \leq 3.5$. Figure 6 presents the transverse momentum dependent purity and acceptance*efficiency for reconstructed D^0 ($\bar{D^0}$) with 0.2 $GeV/c < p_T < 1.0\ GeV/c$.

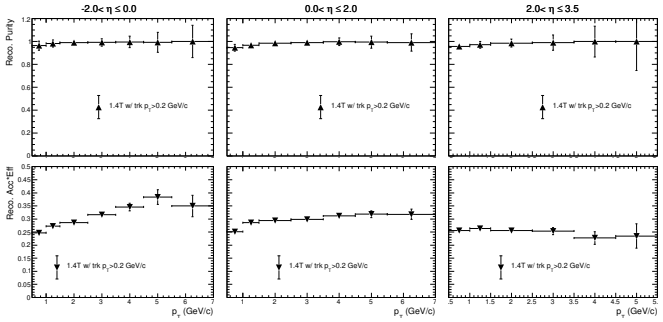

Figure 5: Transverse momentum p_T dependent purity (top) and acceptance*efficiency (bottom) for reconstructed D^0 ($\bar{D^0}$) in three different pseudorapidity regions with the ECCE detector performance in 10+100 GeV $e + p$ collisions. The transverse momentum for reconstructed D^0 ($\bar{D^0}$) is within 0.5 GeV/c to 7 GeV/c region. The integrated luminosity is 10 fb^{-1}.

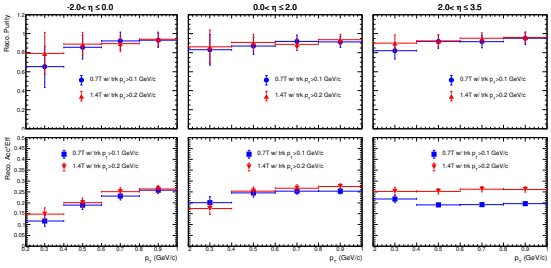

Figure 6: Transverse momentum p_T dependent purity (top) and acceptance*efficiency (bottom) for reconstructed D^0 ($\bar{D^0}$) in three different pseudorapidity regions with the ECCE detector performance in 10+100 GeV $e + p$ collisions. The transverse momentum for reconstructed D^0 ($\bar{D^0}$) is within 0.2 GeV/c to 1 GeV/c region. The integrated luminosity is 10 fb^{-1}.

For jet reconstruction, the anti-k_T algorithm is used and the jet cone radius R is selected as 1.0, where R is $\sqrt{(\eta_{jet} - \eta_{track})^2 + (\phi_{jet} - \phi_{track})^2}$. FIG 7. Initial work has been peroformed in [7], which depends on whether a jet contains a fully reconstructed charm or bottom hadron. To improve the jet tagging efficiency, new jet tagging is developed. It's based on the displaced vertex associated with at least two tracks inside the jet, which matches with a charm hadron or bottom hadron decay vertex within 100 micron. If a jet does not contain a displaced vertex associated with a heavy flavor product decay, then this jet is marked as a light flavor jets. FIG 7 illustrates the transverse momentum distributions of reconstructed jets with different flavors in 10+100 $e + p$ collisions with integrated luminosity at 10 fb^{-1}. Reconstructed efficiencies have been included in the yields presented in FIG 7. Jet purity is under study and will be included later on.

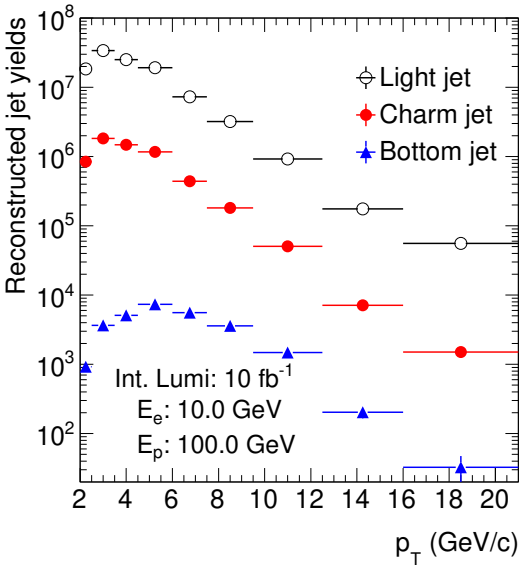

Figure 7: Reconstructed heavy flavor jet transverse momentum p_T distributions with the ECCE detector performance in 10+100 GeV $e + p$ collisions. The integrated luminosity is 10 fb^{-1}.

3. Results

3.1. Flavor dependent R_{eAu}

The flavor dependent nuclear modification factor R_{eAu} have been determined from the extracted reconstructed heavy flavor hadron and jet yields detailed in Chapter 2.2. As we don't have a well defined e+Au event generator yet, the heavy flavor hadron/jet spectrum in $e + Au$ collisions are the nucleus mass number (A) scaling of the related $e + p$ spectrum. The projected hadron momentum fraction z_h dependent R_{eAu} statistical uncertainties with the ECCE detector performance in 10+100 GeV $e + p$ and $e + Au$ collisions are shown in FIG 8.

A different magnet option: Beast magnet has been used to reevaluated the tracking performance with the same detector geometry. The corresponding projected momentum fraction z_h dependent nuclear modification factor R_{eAu} for reconstructed $\pi^{\pm}$, $D^{\pm}$ and $B^{\pm}$ hadrons with the same ECCE detector geometry but with the Beast magnet is shown in Figure 9

The difference between the two magnet options for the projected momentum fraction z_h dependent nuclear modification factor R_{eAu} for reconstructed $\pi^{\pm}$, $D^{\pm}$ and $B^{\pm}$ hadrons are illustrated in Figure 10, where the statistical uncertainties are evaluated with the tracking performance with the ECCE detector and the statistical uncertainty differences are referred to as the difference on the statistical uncertainties with the Babar and the Beast magnet. The change on the projected open heavy flavor hadron nuclear modification factor due to different magnet selections is small.

3.2. Pseudorapidity dependent charm R_{eAu}

The future EIC can provide an ideal environment to explore the hadronization process in vacuum and a cold nuclear medium

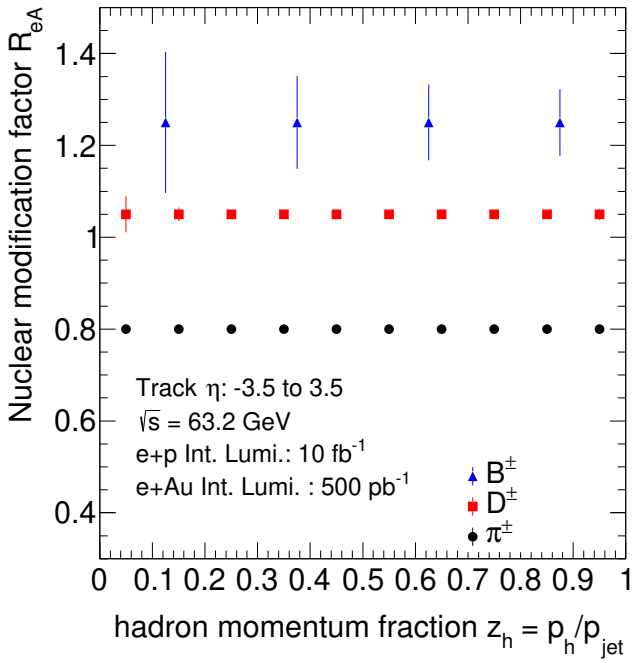

Figure 8: Reconstructed hadron momentum fraction z_h dependent nuclear modification factor R_{eAu} for $\pi^{\pm}$, $D^{\pm}$ and $B^{\pm}$ with the ECCE detector performance in 10+100 GeV $e+p$ and $e+Au$ collisions. The tracking performance is evaluated with the Babar magnet. The integrated luminosity for $e+p$ ($e+Au$) collisions is 10 fb^{-1} (500 pb^{-1}).

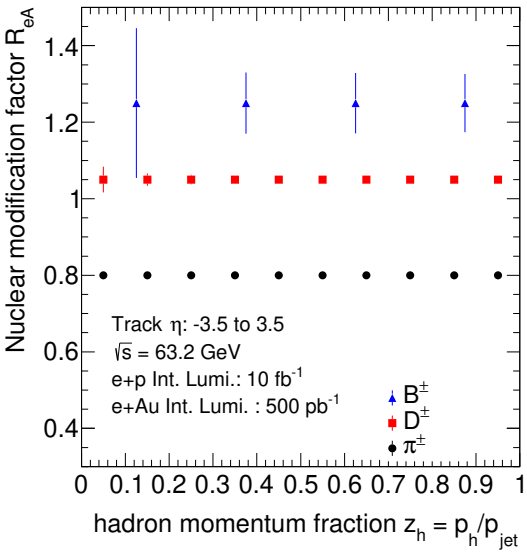

Figure 9: Reconstructed hadron momentum fraction z_h dependent nuclear modification factor R_{eAu} for $\pi^{\pm}$, $D^{\pm}$ and $B^{\pm}$ with the ECCE detector performance in 10+100 GeV $e+p$ and $e+Au$ collisions. The tracking performance is evaluated with the Beast magnet. The integrated luminosity for $e+p$ ($e+Au$) collisions is 10 fb^{-1} (500 pb^{-1}).

through measuring hadron cross section in both $e+p$ and $e+A$ collisions. Recent theoretical developments based on the energy loss mechanism have projected the nuclear modification factor for D-meson and B-meson in $e+Au$ collisions at different center of mass energies [8]. Good statistics in charm production can be achieved at the EIC. With the ECCE detector performance, the projected hadron momentum fraction z_h dependent nuclear modification factor R_{eAu} for reconstructed D^0 ($\bar{D^0}$) in 10+100 GeV $e+p$ and $e+Au$ collisions within the pseudorapidity bins of $-2 < \eta < 0$, $0 < \eta < 2$ and $2\eta < 3.5$ are illustrated in Figure 11. The theoretical predictions based on the parton energy loss model are shown in Figure 11 in the respective pseudorapidity bins. Systematical uncertainties in these measurements include reconstructed D^0 ($\bar{D^0}$) yield variations from different detector designs, different magnet options (Babar VS Beast) and jet cone radius changes.

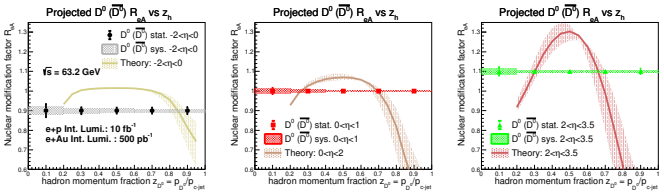

Figure 11: Hadron momentum fraction z_h dependent nuclear modification factor R_{eAu} for reconstructed D^0 ($\bar{D^0}$) with the ECCE detector performance in 10+100 GeV $e+p$ and $e+Au$ collisions. The integrated luminosity for $e+p$ ($e+Au$) collisions is 10 fb^{-1} (500 pb^{-1}). The systematical uncertainties come from different detector design and magnet options. The theoretical calculations are from [8].

Figure 12 presents projected hadron momentum fraction z_h dependent nuclear modification factor R_{eAu} for reconstructed D^0 ($\bar{D^0}$) in 10+100 GeV $e+p$ and $e+Au$ collisions with the ECCE detector performance with both Babar and Beast magnet options within the pseudorapidity bins of $-2 < \eta < 0$, $0 < \eta < 2$ and $2 < \eta < 3.5$. As presented in Figure 11 and

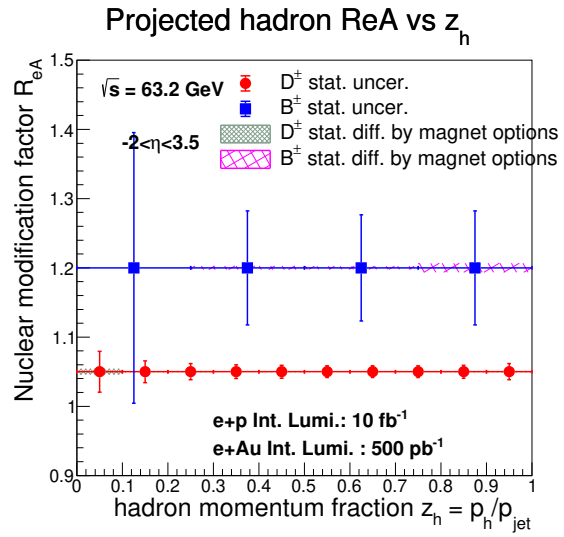

Figure 10: Reconstructed hadron momentum fraction z_h dependent nuclear modification factor R_{eAu} for $\pi^{\pm}$, $D^{\pm}$ and $B^{\pm}$ with the ECCE detector performance in 10+100 GeV $e+p$ and $e+Au$ collisions.

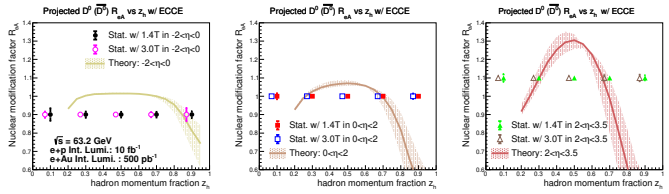

Figure 12: Hadron momentum fraction z_h dependent nuclear modification factor R_{eAu} for reconstructed D^0 ($\bar{D^0}$) with the ECCE detector performance in 10+100 GeV $e+p$ and $e+Au$ collisions. The integrated luminosity for $e+p$ ($e+Au$) collisions is 10 fb^{-1} (500 pb^{-1}). The statistical uncertainties of the projected R_{eAu} with the ECCE detector performance using the 1.4 T Babar (3.0 T Beast) magnet are shown in closed (open) markers. The theoretical calculations are from [8].

Figure 12, better experimental precision can be obtained with the ECCE detector design for reconstructed D^0 ($\bar{D^0}$) R_{eAu} projections compared to the theoretical uncertainties. As the reconstructed hadron pseudorapidity changes from backward going direction to the forward going direction, the projected D^0 ($\bar{D^0}$) R_{eAu} based on the parton energy loss model has a enhancement trend. Unlike the parton energy loss model, the absorption model indicates that the heavy flavor R_{eA} should be less than 1. With the precision provied by the ECCE detector, good discriminating power will be provided by the open heavy flavor R_{eA} measurements in separating different model predictions.

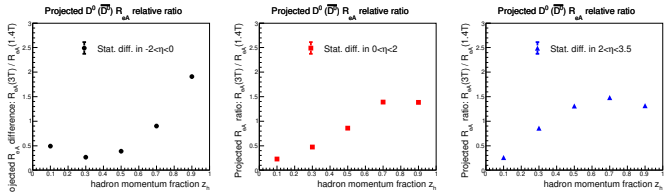

Figure 13: Statistical uncertainty difference in the hadron momentum fraction z_h dependent nuclear modification factor R_{eAu} for reconstructed D^0 ($\bar{D^0}$) with the ECCE detector performance in 10+100 GeV $e+p$ and $e+Au$ collisions. The statistical uncertainty ratio of the projected R_{eAu} is defined as the R_{eAu} statistical uncertainty with the 3.0 T Beast magnet over that using the 1.4 T Babar magnet.The integrated luminosity for $e+p$ ($e+Au$) collisions is 10 fb^{-1} (500 pb^{-1}).

The relative ratio which is defined as the statistical uncertainty of the projected R_{eAu} of reconstructed D^0 ($\bar{D^0}$) with the 3T Beast magnetic field over the projected uncertainty with the 1.5 T Babar magnetic field in the three different pseudorapidity regions are illustrated in Figure 13. For the low hadron momentum fraction

4. Acknowledgements

We thank the many individuals and funding agencies which provided important advice and support for this work.

References

[1] R. Abdul Khalek, et al., Science Requirements and Detector Concepts for the Electron-Ion Collider: EIC Yellow Report (3 2021). arXiv:2103.05419.

[2] T. Sjöstrand, S. Ask, J. R. Christiansen, R. Corke, N. Desai, P. Ilten, S. Mrenna, S. Prestel, C. O. Rasmussen, P. Z. Skands, An introduction to PYTHIA 8.2, Comput. Phys. Commun. 191 (2015) 159–177. arXiv:1410.3012, doi:10.1016/j.cpc.2015.01.024.

[3] S. Agostinelli, et al., Geant4—a simulation toolkit, Nuclear Instruments and Methods in Physics Research Section A: Accelerators, Spectrometers, Detectors and Associated Equipment 506 (3) (2003) 250–303. doi:https://doi.org/10.1016/S0168-9002(03)01368-8.

[4] J. Arrington, et al., EIC Physics from An All-Silicon Tracking Detector (2 2021). arXiv:2102.08337.

[5] X. Li, et al., A New Heavy Flavor Program for the Future Electron-Ion Collider, EPJ Web Conf. 235 (2020) 04002. arXiv:2002.05880, doi:10.1051/epjconf/202023504002.

[6] C.-P. Wong, X. Li, M. Brooks, M. J. Durham, M. X. Liu, A. Morreale, C. da Silva, W. E. Sondheim, A Proposed Forward Silicon Tracker for the Future Electron-Ion Collider and Associated Physics Studies (9 2020). arXiv:2009.02888.

[7] X. Li, Heavy flavor and jet studies for the future Electron-Ion Collider, PoS HardProbes2020 (2021) 175. arXiv:2007.14417, doi:10.22323/1.387.0175.

[8] H. T. Li, Z. L. Liu, I. Vitev, Heavy meson tomography of cold nuclear matter at the electron-ion collider, Phys. Lett. B 816 (2021) 136261. arXiv:2007.10994, doi:10.1016/j.physletb.2021.136261.